SIAM J. APPLIED DYNAMICAL SYSTEMS
Vol. 8, No. 4, pp. 1632–1663

Computer Assisted Proof of the Existence of Homoclinic Tangency for the Hénon Map and for the Forced Damped Pendulum*

Daniel Wilczak† and Piotr Zgliczyński‡

Abstract. We present a topological method for the efficient computer assisted verification of the existence of the homoclinic tangency which unfolds generically in a one-parameter family of planar maps. The method has been applied to the Hénon map and the forced damped pendulum ODE.

Key words. homoclinic tangency, covering relation, cone condition, transversal intersection, computer assisted proof

AMS subject classifications. Primary, 37M20; Secondary, 34C37, 37N30

DOI. 10.1137/090759975

1. Introduction.

The goal of our paper is to describe a method for the verification of the existence of the quadratic homoclinic tangency which unfolds generically in a one-parameter family of planar maps. This is an important problem problem in dynamics, because establishing the existence of the generic homoclinic tangency has very deep dynamical consequences; see, for example, [14, 17, 18, 15] and references therein.

Our paper was inspired by the works of Arai and Mischaikow [1, 2], who combined some tools from the Conley index theory, the tools of computational homology from *the CHOMP project* [4], and the set oriented numerical methods from *the GAIO project* [5], into a method for computer assisted proof of the existence of the generic homoclinic tangency. Using it, they proved in [2] the existence of the generic homoclinic tangency for the dissipative Hénon map $H_{a,b}(x, y) = (a - x^2 + by, x)$ for parameter values close to $a = 1.4$, $b = 0.3$ and $a = 1.3$, $b = -0.3$. Their method contains essentially two separate parts: first, using the Conley index approach, they prove the existence of the homoclinic tangency for some parameter value (steps 1 to 5 in the terminology used in [2]), and in the second part (step 6 in [2]) they verify some transversality-type condition, which implies the genericity of the homoclinic tangency established in the first part. The computation times reported in [2] are around 260 minutes and 100 minutes on a PowerMac G5 (2GHz) for $b = 0.3$ and $b = -0.3$, respectively. In these computations the second part took 61 minutes and 24 minutes, respectively. From these computation times it is quite clear that there is little hope of successfully applying this method to ODEs.

*Received by the editors May 24, 2009; accepted for publication (in revised form) by H. Kokubu September 7, 2009; published electronically December 9, 2009. This research was supported in part by the Polish State Ministry of Science and Information Technology grant N201 024 31/2163.
http://www.siam.org/journals/siads/8-4/75997.html
†Department of Mathematics, University of Bergen, Johannes Brunsgate 12, 5008 Bergen, Norway (wilczak@ii.uj.edu.pl).
‡Jagiellonian University, Institute of Computer Science, Łojasiewicza 6, 30-348 Kraków, Poland (zgliczyn@ii.uj.edu.pl).

Our method, also topological and geometric in spirit, is based on the observation that the computations done by Arai and Mischaikow in [2] in the second part of their approach should be in principle sufficient to obtain the whole result—both the existence of the homoclinic tangency and its genericity. Obviously, for this end, one should use different tools; ours are essentially those of differential topology but were developed earlier in the context of topological dynamics, such as the covering relations combined with the cone conditions; see [12, 22]. As a test case we give a computer assisted proof of the existence of the generic homoclinic tangency for the dissipative Hénon map with $b = -0.3$ and $a \approx 1.3145$ in the computation time 0.2 sec on the Intel Xeon 5160, 3GHz processor. This should be contrasted with the fact that in [2] this case took around 100 minutes.

An application of our method to an ODE requires an efficient rigorous C^2-solver for ODEs. By this we mean an algorithm for rigorous integration of ODEs together with their variational equations up to the second order. Such an algorithm has been recently developed by the authors in [21] and is now a part of the CAPD library [8]. Using this algorithm, we were able to prove the existence of the generic homoclinic tangency for the 2π-shift along the trajectory of the periodically forced pendulum equation

$$\ddot{x} + \beta\dot{x} + \sin(x) = \cos(t) \tag{1.1}$$

for $\beta \approx 0.2471$ (see Theorem 7.1 in section 7). The computation time for this proof is 30 sec on the Intel Xeon 5160, 3GHz processor.

It should be mentioned that similar results for the Hénon map have been obtained by a complex analytic method of Fornaess and Gavosto [6, 7]. Compared to their method, which depends on the analyticity of maps, our method and that of Arai and Mischaikow are rather geometric and topological and are designed so that they can be applied to a wider class of maps. Essentially, we require a continuous family of C^2 diffeomorphisms for which we can compute the image of the maps using interval arithmetic.

The content of the paper may be briefly described as follows: in sections 2 and 3, following mainly [2], we give basic definitions and restate the problem of the existence of the quadratic homoclinic tangency unfolding generically as the transversality question for a dynamical system induced by the given one on the projective bundle. In section 4 we discuss how this transversality problem can be solved using the covering relations linked with the cone conditions. Moreover, we derive computable estimates for the dependence on a parameter of (un)stable manifolds of the hyperbolic fixed point, which will be used later in the computer assisted proofs. In section 5 we illustrate our approach on a toy example, with the intention that the reader may see and appreciate some details of the method, which are later hardly visible when we report on the computer assisted proof for the Hénon map and for the forced damped pendulum in sections 6 and 7, respectively.

2. Homoclinic tangency and the projectivization.

2.1. Invariant manifold—basic notation.

Definition 2.1. *Consider the map $f : X \supset \mathrm{dom}(f) \to X$. Let $x \in X$. Any sequence $\{x_k\}_{k\in I}$, where $I \subset \mathbb{Z}$ is a set containing 0 and for any $l_1 < l_2 < l_3$ in $\mathbb{Z}$ if $l_1, l_3 \in I$, then $l_2 \in I$, such that*

$$x_0 = x, \qquad f(x_i) = x_{i+1} \qquad \text{for } i, i+1 \in I,$$

will be called an orbit through x. If $I = \mathbb{Z}_-$, then we will say that $\{x_k\}_{k\in I}$ is a full backward orbit through x.

Definition 2.2. *Let X be a topological space and let the map $f : X \supset \mathrm{dom}\,(f) \to X$ be continuous.*

Let $Z \subset \mathbb{R}^n$, $x_0 \in Z$, $Z \subset \mathrm{dom}\,(f)$. We define

$$\begin{aligned}
W^s_Z(z_0, f) &= \{z \mid \forall_{n\geq 0} f^n(z) \in Z, \quad \lim_{n\to\infty} f^n(z) = z_0\},\\
W^u_Z(z_0, f) &= \{z \mid \exists\ \{x_n\} \subset Z \text{ a full backward orbit through } z, \text{ such that}\\
&\qquad \lim_{n\to -\infty} x_n = z_0\},\\
W^s(z_0, f) &= \{z \mid \lim_{n\to\infty} f^n(z) = z_0\},\\
W^u(z_0, f) &= \{z \mid \exists\ \{x_n\} \text{ a full backward orbit through } z, \text{ such that}\\
&\qquad \lim_{n\to -\infty} x_n = z_0\}.
\end{aligned}$$

If f is known from the context, then we will usually drop it and use $W^s(z_0)$, $W^s_Z(z_0)$, etc., instead.

2.2. Projectivization of the dynamics. The notation and setting are those used in [2]. Let $f : X \to X$ be a diffeomorphism of a manifold X.

Definition 2.3. *Let $z_0 \in X$. We say that z_0 is a* hyperbolic fixed point for f *iff $f(z_0) = z_0$ and $Sp(Df(z_0)) \cap S^1 = \emptyset$, where $Df(z_0)$ is the derivative of f at z_0 and $Sp(A)$ denotes the spectrum of a square matrix A.*

We denote the tangent bundle of X by TX and the differential of f by Df. From the dynamical system $f : X \to X$ we can derive a new dynamical system $Pf : PX \to PX$, which is defined as follows. The space PX is the projective bundle associated to the tangent bundle of X, that is, the fiber bundle on X whose fiber over $x \in X$ is the projective space of T_xX. That is,

$$PX = \bigcup_{x\in X} P_xX := \bigcup_{x\in X} \{\text{one-dimensional subspace of } T_xX\}.$$

For a submanifold S in X by PS we will denote its projectivization, which is given by

$$PS = \{(x, [v]) \in PX \mid x \in S, v \in T_xS \setminus \{0\}\}.$$

It is easy to see that $P(S)$ is a manifold and $\dim(P(S)) = 2\dim(S) - 1$.

Define Pf to be the map induced from Df on PX, namely, $Pf(x, [v]) := (f(x), [Df(x)\cdot v])$, where $0 \neq v \in T_xX$, $[v]$ is the subspace in T_xX spanned by v, and $Df(x) : T_xX \to T_{f(x)}X$ is the derivative of f at x. The geometry of projectivization in the case of $f : \mathbb{R}^2 \to \mathbb{R}^2$ is shown in Figure 1.

Let us identify X with the zero section of TX. We define the map $\pi : TX \setminus X \to PX$ by $\pi((x, v)) = (x, [v])$ for $x \in X$, $v \in T_xX$.

Let $p \in X$ be a hyperbolic fixed point of f and let $T_pX = \tilde{E}^s_p \oplus \tilde{E}^u_p$ be the corresponding splitting of the tangent space into stable and unstable subspaces for $Df(p)$. Define $E^s_p := \pi(\tilde{E}^s_p \setminus \{0\})$ and $E^u_p := \pi(\tilde{E}^u_p \setminus \{0\})$.

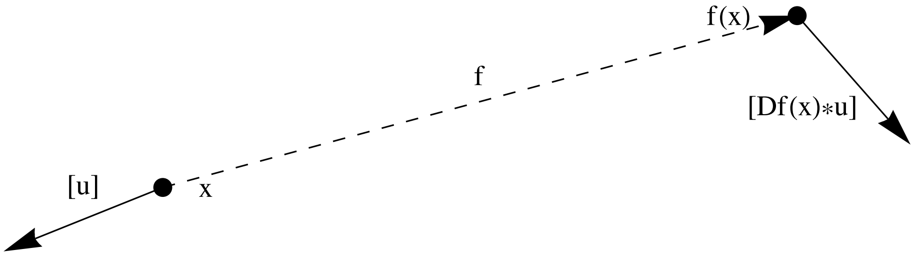

Figure 1. *The geometry of projectivization. The map Pf maps a point x to $f(x)$ and a subspace of T_xX spanned by u into a subspace of $T_{f(x)}X$ spanned by $Df(x)\cdot u$.*

2.3. Dimension two.

Theorem 2.4. *Let $f:\mathbb{R}^2\to\mathbb{R}^2$ be a diffeomorphism and let p be a hyperbolic fixed point with one-dimensional stable and unstable manifolds.*

Then

1. (p,E^u_p) *is a hyperbolic fixed point for Pf such that*
   - $W^u((p,E^u_p),Pf)=P(W^u(p,f))$, $\dim W^u((p,E^u_p),Pf)=1$,
   - $W^s((p,E^u_p),Pf)=\{(z,[v])\in PX \mid z\in W^s(p,f),(z,[v])\notin P(W^s(p,f))\}$, $\dim W^s((p,E^u_p),Pf)=2$.
2. (p,E^s_p) *is a hyperbolic fixed point for Pf such that*
   - $W^s((p,E^s_p),Pf)=P(W^s(p,f))$, $\dim W^s((p,E^s_p),Pf)=1$,
   - $W^u((p,E^s_p),Pf)=\{(z,[v])\in PX \mid z\in W^u(p,f),(z,[v])\notin P(W^u(p,f))\}$, $\dim W^u((p,E^s_p),Pf)=2$.

Proof. It is easy to see that the stable and unstable sets are as stated. There remains for us to show the hyperbolicity only. Consider first (p,E^u_p). Let us change the coordinate system in $\mathbb{R}^2$ such that $p=0$ and $Df(p)$ is diagonal,

$$Df(p)=\begin{pmatrix}\lambda & 0\\ 0 & \mu\end{pmatrix},$$

where $|\lambda|>1$ and $|\mu|<1$. From now on all considerations will be done in this coordinate frame.

Around $(p,E^u(p))$ we will use the coordinate system $\varphi:\mathbb{R}^2\times\mathbb{R}\to P(\mathbb{R}^2)$ given by

$$\varphi(z,v)=(z,[(1,v)]).$$

It is easy to see that

$$\varphi^{-1}(z,[(v_1,v_2)])=(z,v_2/v_1).$$

In these coordinates (p,E^u_p) is given by $(0,0)$. Now we compute the linearization of Pf around $(0,0)$.

We have

$$Pf(z,v)=(f(z),[Df(z)\cdot(1,v)^T])=(Df(0)\cdot z+o(|z|),[Df(z)\cdot(1,v)^T]).$$

Observe that

$$
\begin{aligned}
Df(z)\cdot(1,v)^T &= \begin{pmatrix} \frac{\partial f_1}{\partial x}(z) & \frac{\partial f_1}{\partial y}(z) \\ \frac{\partial f_2}{\partial x}(z) & \frac{\partial f_2}{\partial y}(z) \end{pmatrix} \cdot \begin{pmatrix} 1 \\ v \end{pmatrix} = \begin{pmatrix} \lambda & 0 \\ 0 & \mu \end{pmatrix} \cdot \begin{pmatrix} 1 \\ v \end{pmatrix} \\
&+ \begin{pmatrix} \frac{\partial^2 f_1}{\partial x^2}(0)x + \frac{\partial^2 f_1}{\partial x \partial y}(0)y & \frac{\partial^2 f_1}{\partial y \partial x}(0)x + \frac{\partial^2 f_1}{\partial y^2}(0)y \\ \frac{\partial^2 f_2}{\partial x^2}(0)x + \frac{\partial^2 f_2}{\partial x \partial y}(0)y & \frac{\partial^2 f_2}{\partial y \partial x}(0)x + \frac{\partial^2 f_2}{\partial y^2}(0)y \end{pmatrix} \cdot \begin{pmatrix} 1 \\ v \end{pmatrix} + o(z) \cdot \begin{pmatrix} 1 \\ v \end{pmatrix} \\
&= \begin{pmatrix} \lambda + O(|(z,v)|) \\ \mu v + \frac{\partial^2 f_2}{\partial x^2}(0)x + \frac{\partial^2 f_2}{\partial x \partial y}(0)y + o(|(z,v)|) \end{pmatrix}.
\end{aligned}
$$

Now we have to divide the second component of the above vector by the first one. Therefore,

$$
\begin{aligned}
v_2/v_1 &= \left(\mu v + \frac{\partial^2 f_2}{\partial x^2}(0)x + \frac{\partial^2 f_2}{\partial x \partial y}(0)y + o(|(z,v)|)\right) \cdot \lambda^{-1}(1 + O(|(z,v)|) \\
&= \frac{\mu}{\lambda} v + \frac{1}{\lambda}\frac{\partial^2 f_2}{\partial x^2}(0)x + \frac{1}{\lambda}\frac{\partial^2 f_2}{\partial x \partial y}(0)y + o(|(z,v)|).
\end{aligned}
$$

We have proved that the linearization of Pf at $p = (0,0)$ has the following form:

$$
DPf(p, E^u_p) = \begin{pmatrix} \lambda & 0 & 0 \\ 0 & \mu & 0 \\ \frac{1}{\lambda}\frac{\partial^2 f_2}{\partial x^2}(0) & \frac{1}{\lambda}\frac{\partial^2 f_2}{\partial x \partial y}(0) & \frac{\mu}{\lambda} \end{pmatrix}.
$$

Hence we see that (p, E^u_p) is a hyperbolic fixed point for Pf with one-dimensional unstable and two-dimensional stable manifolds.

Let us consider now (p, E^s_p). This time we will use the coordinate system $\varphi : \mathbb{R}^2 \times \mathbb{R} \to P(\mathbb{R}^2)$ given by

$$
\varphi(z, v) = (z, [(v, 1)]).
$$

It is easy to see that

$$
\varphi^{-1}(z, [(v_1, v_2)]) = (z, v_1/v_2).
$$

Similar computations lead to the following formula for the linearization of Pf at (p, E^s_p):

$$
DPf(p, E^s_p) = \begin{pmatrix} \lambda & 0 & 0 \\ 0 & \mu & 0 \\ \frac{1}{\mu}\frac{\partial^2 f_1}{\partial x \partial y}(0) & \frac{1}{\mu}\frac{\partial^2 f_1}{\partial y^2}(0) & \frac{\lambda}{\mu} \end{pmatrix}. \qquad \blacksquare
$$

From Theorem 2.4 we obtain the following remark.

Remark 2.5. *If f is as in Theorem 2.4 and $W^s(p,f)$ and $W^u(p,f)$ have a nonempty intersection, then*

- *if $W^s(p,f)$ and $W^u(p,f)$ are tangent, then we obtain a heteroclinic connection from (p, E^u_p) to (p, E^s_p);*
- *if $W^s(p,f)$ and $W^u(p,f)$ intersect transversally, then we obtain a homoclinic connection from (p, E^u_p) to (p, E^u_p).*

3. Generic unfolding of quadratic tangency as the transversality question. We assume that we have two curves in $\mathbb{R}^2$ depending on some parameter a and given by $u(a,t) = (f_1(a,t), f_2(a,t))$ and $s(a,t) = (g_1(a,t), g_2(a,t))$. We are interested in establishing conditions, which will imply the existence of the generic unfolding of the quadratic tangency between them. Our goal is to formulate such conditions as the transversality question. This is Theorem 2.1 from [2], where it was stated without proof.

Definition 3.1 (see [14, section 3.1]). *Let $I, J, Z \subset \mathbb{R}$ be intervals. Let $u_\mu \colon I \to \mathbb{R}^2$ and $s_\mu \colon J \to \mathbb{R}^2$ for $\mu \in Z$ be two smooth curves depending on μ in the smooth way, such that $u_{\mu_0}(t_u) = s_{\mu_0}(t_s) = q_0$ and u and s are tangent at q_0.*

Assume there exist μ-dependent coordinates in a neighborhood of q for μ close to μ_0, such that in these coordinates we can use x_1 (the first coordinate) as the parameter of our curves and the following hold:

$$\begin{aligned} s_\mu(x_1) &= (x_1, 0), \\ u_\mu(x_1) &= (x_1, ax_1^2 + b(\mu - \mu_0)), \end{aligned} \tag{3.1}$$

where $a \neq 0, b \neq 0$. Then we say that the quadratic tangency of u and s unfolds generically*.*

Remark 3.2. *It is easy to see that in the above definition we can exchange the role of curves u and s using the coordinate transformation given by $\phi_\mu(x_1, x_2) = (x_1, x_2 - ax_1^2 - b(\mu - \mu_0))$.*

Remark 3.3. *In the context of Definition 3.1, if $u_\mu(x_1) = g(\mu, x_1)$, then instead of (3.1) it is enough to require*

$$\begin{aligned} g(\mu_0, 0) = 0, &\quad \frac{\partial g}{\partial x_1}(\mu_0, 0) = 0, \\ \frac{\partial g}{\partial \mu}(\mu_0, 0) \neq 0, &\quad \frac{\partial^2 g}{\partial x_1^2}(\mu_0, 0) \neq 0. \end{aligned}$$

The proof of Remark 3.3 will be given in Appendix A.

Theorem 3.4. *Let $\Lambda \subset \mathbb{R}$ be an interval. Let $u : \Lambda \times \mathbb{R} \to \mathbb{R}^2$ and $s : \Lambda \times \mathbb{R} \to \mathbb{R}^2$ be two C^2-curves depending on parameter $a \in \Lambda$. Let $a_0 \in \Lambda$ be a parameter at which curves u_a and s_a are tangent.*

These curves have a quadratic tangency at a_0 which unfolds generically iff there exist $t_u, t_s \in \mathbb{R}$, such that surfaces

$$E(u), E(s) : \Lambda \times \mathbb{R} \to \mathbb{R}^3 \times R\mathbb{P}^1$$

given by

$$\begin{aligned} E(u)(a,t) &= \left(a, u(a,t), \left[\frac{\partial u}{\partial t}(a,t)\right]\right), \\ E(s)(a,t) &= \left(a, s(a,t), \left[\frac{\partial s}{\partial t}(a,t)\right]\right) \end{aligned}$$

intersect transversally at the point $E(u)(a_0, t_u) = E(s)(a_0, t_s)$.

Before the proof we need one lemma.

Lemma 3.5. *Let* $s = (s_1, s_2) : \Lambda \times \mathbb{R} \to \mathbb{R}^2$ *be a* C^2*-map, such that* $\frac{\partial s_1}{\partial t}(a_0, t_0) \neq 0$ *for some* (a_0, t_0).

Then there exist a neighborhood Λ' *of* a_0*, an open set* V*, such that* $s(a_0, t_0) \in V$*, and* a*-dependent coordinates on* V *for* $a \in \Lambda'$*, i.e.,* $\phi_a : V \to \mathbb{R}^2$ *for* $a \in \Lambda'$*, such that after a suitable reparameterization in these new coordinates the mapping* s *has locally the following form:*

$$s(a, t) = (t, 0).$$

Proof. Let us denote by (x, y) coordinates in $\mathbb{R}^2$. By taking a suitable parameterization and shifting the coordinates' origin and permuting, if necessary, the coordinates in $\mathbb{R}^2$, we can assume that $t_0 = 0$, $s(a_0, 0) = 0$, and $\frac{\partial s_1}{\partial t}(a_0, 0) > 0$. We can locally (in a suitable open set U) use x as the parameter of a curve $s(a, \cdot)$ for $a \in \tilde{\Lambda} \subset \Lambda$. Therefore, we have

$$s(a, t) = (t, s_2(a, t)).$$

Consider the map $\varphi : \tilde{\Lambda} \times U \to \tilde{\Lambda} \times \mathbb{R}^2$ given by

$$\varphi(a, x, y) = (a, x, y - s_2(a, x)).$$

We have

$$D\varphi(a, x, y) = \begin{bmatrix} 1 & 0 & 0 \\ 0 & 1 & 0 \\ -\frac{\partial s_2}{\partial a}(a, x) & -\frac{\partial s_2}{\partial x}(a, x) & 1 \end{bmatrix}.$$

Therefore, φ is a local diffeomorphism. Let open sets Λ', V be such that $\varphi : \Lambda' \times V \to \Lambda' \times \mathbb{R}^2$ is a diffeomorphism on the image and $(a_0, 0) \in \Lambda' \times V$. The a-dependent coordinates on V are given by $\phi_a(x, y) = \varphi(a, x, y)$.

It is easy to see that in the new coordinates given by ϕ_a the curve s has the following form:

$$s(a, t) = (t, 0). \qquad \blacksquare$$

Proof of Theorem 3.4. By Lemma 3.5 we can assume that the curve s is given by

$$s(a, t) = (t, 0).$$

Observe that the transversality implies that in the neighborhood of the intersection point the curve u can be represented as

$$u(a, t) = (t, g_2(a, t)),$$

where g_2 satisfies the following conditions:

$$g_2(a_0, 0) = 0, \quad \frac{\partial g_2}{\partial t}(a_0, 0) = 0. \tag{3.2}$$

Now we will prove that the transversality of $E(u)$ and $E(s)$ is equivalent to

$$\frac{\partial g_2}{\partial a}(a_0, 0) \neq 0,$$
$$\frac{\partial^2 g_2}{\partial t^2}(a_0, 0) \neq 0.$$

Observe that from Remark 3.3 it follows that the above conditions together with (3.2) are equivalent to the generic unfolding of the quadratic tangency.

Observe that $\frac{\partial s}{\partial t}(a,t) = (1,0)$ and $\frac{\partial u}{\partial t}(a_0, t=0) = (1,0)$; therefore, in the neighborhood of $[\frac{\partial s}{\partial t}(a,t)]$ we can use the second coordinate as a chart map in $R\mathbb{P}^1$.

In these coordinates we have

$$E(s)(a,t) = (a,t,0,0)^T,$$
$$E(u)(a,t) = \left(a, t, g_2(a,t), \frac{\partial g_2}{\partial t}(a,t)\right)^T.$$

We have

$$T_{E(s)(a_0,t=0)} = \operatorname{span}\begin{pmatrix} 1 & 0 \\ 0 & 1 \\ 0 & 0 \\ 0 & 0 \end{pmatrix}$$

and

$$T_{E(u)(a_0,t=0)} = \operatorname{span}\begin{pmatrix} 1 & 0 \\ 0 & 1 \\ \frac{\partial g_2}{\partial a}(a_0,0) & \frac{\partial g_2}{\partial t}(a_0,0) \\ \frac{\partial^2 g_2}{\partial t \partial a}(a_0,0) & \frac{\partial^2 g_2}{\partial t^2}(a_0,0) \end{pmatrix}.$$

From (3.2) it follows that the transversality question is equivalent to the following determinant being nonzero:

$$\det\begin{pmatrix} 1 & 0 & 1 & 0 \\ 0 & 1 & 0 & 1 \\ 0 & 0 & \frac{\partial g_2}{\partial a}(a_0,0) & 0 \\ 0 & 0 & \frac{\partial^2 g_2}{\partial t \partial a}(a_0,0) & \frac{\partial^2 g_2}{\partial t^2}(a_0,0) \end{pmatrix} = \frac{\partial g_2}{\partial a}(a_0,0) \cdot \frac{\partial^2 g_2}{\partial t^2}(a_0,0).$$

This finishes the proof. ■

4. How to prove the homoclinic tangency using the covering relations and the cone conditions? We assume that the reader is familiar with the following notions: h-sets, covering relations, cone conditions, and horizontal and vertical disks as defined in [12, 22].

We consider a planar map $f_a : \mathbb{R}^2 \supset \operatorname{dom}(f) \to \mathbb{R}^2$ depending on the parameter a, which has a hyperbolic fixed point p_a with one-dimensional unstable and stable manifolds. Hence according to the setting from section 2 we will work in four-dimensional space, using coordinates (a, x, y, v), where a is the parameter, $(x, y) \in \mathbb{R}^2$, and v represents points in $P(T_{(x,y)}\mathbb{R}^2)$, which we will call the *tangential* coordinate. We have the map (we abuse the notation for Pf)

$$Pf(a,x,y,v) = (a, Pf(x,y,v)).$$

In our method we need the following ingredients:

- the chain of covering relations

$$N_0 \overset{Pf}{\Longrightarrow} N_1 \overset{Pf}{\Longrightarrow} \cdots \overset{Pf}{\Longrightarrow} N_k, \tag{4.1}$$

  such that the cone conditions are satisfied,

- $(a, W^u((p_a, E^u_{p_a}), Pf_a))$ as the horizontal disk in N_0 satisfying the cone conditions,
- $(a, W^s((p_a, E^s_{p_a}), Pf_a))$ as the vertical disk in N_k satisfying the cone conditions.

If the above conditions are satisfied, then from [22, Theorem 7] it follows that $(a, W^u((p_a, E^u_{p_a}), Pf_a))$ contains a horizontal disk satisfying the cone conditions in N_k. Hence $(a, W^u((p_a, E^u_{p_a}), Pf_a))$ and $(a, W^s((p_a, E^s_{p_a}), Pf_a))$ intersect transversally in N_k, which by Theorem 3.4 implies that sets $W^u((p_a, E^u_{p_a}), Pf_a)$ and $W^s((p_a, E^s_{p_a}), Pf_a)$ have a quadratic tangency which unfolds generically.

Since the parameter a is not changing under Pf, apparently there is a problem with the realization of the above scenario, because the covering relations together with the cone conditions imply the hyperbolicity. The essential point is that this remark is valid for closed loops of covering relations, but in our setting we just want a chain of covering relations going from one part of our phase space to another. While constructing such a chain we will arbitrarily decide whether we treat the parameter as the "unstable" or "stable" direction by simply adjusting the sizes of the h-sets in a-direction.

To make our scheme working we need the following:

- We need to set the dimensions u, s in our h-sets N_i to be equal to 2, because this is the dimension of $(a, W^u((p_a, E^u_{p_a}), Pf_a))$ and $(a, W^s((p_a, E^s_{p_a}), Pf_a))$.
- $(a, W^u((p_a, E^u_{p_a}), Pf_a))$ should be a horizontal disk in N_0; hence we should treat a as one of the unstable directions.
- $(a, W^s((p_a, E^s_{p_a}), Pf_a))$ should be a vertical disk in N_k; hence we should treat a as one of the stable directions.

4.1. The Lipschitz dependence of stable and unstable manifolds on parameters. We need to prove that $(a, W^u((p, E^u_p), Pf_a))$ is a horizontal disk in a suitable h-set N_0; this requires at least the Lipschitz dependence on a of the invariant manifold. In [22, sec. 8.2] the Lipschitz dependence of (un)stable manifolds with respect to parameters with explicit and computable constants was discussed with an eye toward the computer assisted proofs. Here we will just recall these results and refine some estimates given there.

We will be using the norms for quadratic forms (identified in what follows with symmetric matrices) which are defined by

$$|B(u, v)| \le \|B\| \|u\| \|v\|.$$

For the Euclidean norm we have

$$\|B\| = \max\{|s| \mid s \text{ in an eigenvalue of } B\}.$$

Theorem 4.1. *Assume that (N, Q) is an h-set in $\mathbb{R}^{u+s}$ with cones and $f_\lambda\colon \mathbb{R}^{u+s} \to \mathbb{R}^{u+s}$ with $\lambda \in C$, where C is a compact interval in the parameter space and Q has the form $Q(x, y) = \alpha(x) - \beta(y) = \sum_{i=1}^{u} a_i x_i^2 - \sum_{i=1}^{s} a_{i+u} y_i^2$.*

1. *Assume that for the covering relation $N \overset{f_\lambda}{\Longrightarrow} N$ the cone condition is satisfied for all $\lambda \in C$.*
2. *Let $\epsilon > 0$ and $A > 0$ be such that for all $\lambda \in C$ and $z_1, z_2 \in N$ the following holds:*

$$Q(f_\lambda(z_1) - f_\lambda(z_2)) - (1 + \epsilon) Q(z_1 - z_2) \ge A(z_1 - z_2)^2. \tag{4.2}$$

3. *Let*

$$M = \max_{\lambda\in C, z\in N}\left(\sum_i |a_i| \left\|\frac{\partial \pi_{z_i} f_\lambda}{\partial z}(z)\right\| \cdot \left\|\frac{\partial \pi_{z_i} f_\lambda}{\partial \lambda}(z)\right\|\right), \tag{4.3}$$

$$L = \|\beta\| \cdot \max_{\lambda\in C, z\in N} \left\|\frac{\partial \pi_y f_\lambda}{\partial \lambda}(z)\right\|^2. \tag{4.4}$$

4. *Let* $\Gamma > 0$ *be such that*

$$A - 2M\Gamma - L\Gamma^2 > 0. \tag{4.5}$$

5. *We define*

$$\delta = \frac{\Gamma^2}{\|\alpha\|}. \tag{4.6}$$

Then the set $W^s_N(p_\lambda, f_\lambda)$ *for* $\lambda \in C$ *can be parameterized as a vertical disk in* $C \times N$ *for the quadratic form* $\tilde{Q}(\lambda, z) = \delta Q(z) - \lambda^2$.

Before the proof let us make two observations concerning constants A, ϵ, Γ.

Remark 4.2. *The existence of* A *and* ϵ *in* (4.2) *is a consequence of the cone condition for covering relation* $N \overset{f_\lambda}{\Longrightarrow} N$. *We would like to have* A *as big as possible. This forces* $\epsilon \to 0$, *but* ϵ *is not used in what follows.*

Remark 4.3. *Since* $A > 0$, *therefore* Γ *in* (4.5) *always exists, but it is desirable to look for the largest* Γ *possible.*

Proof of Theorem 4.1. We would like to obtain that for $|\lambda_1-\lambda_2| \le \Gamma\|z_1-z_2\|$ the following holds:

$$Q(f_{\lambda_1}(z_1) - f_{\lambda_2}(z_2)) > (1+\epsilon)Q(z_1 - z_2).$$

Let B be a unique symmetric form, such that $B(u,u) = Q(u)$. Observe that

$$\begin{aligned} & Q(f_{\lambda_1}(z_1) - f_{\lambda_2}(z_2)) - (1+\epsilon)Q(z_1 - z_2) \\ = {} & Q(f_{\lambda_1}(z_1) - f_{\lambda_1}(z_2)) - (1+\epsilon)Q(z_1 - z_2) \\ & + 2B(f_{\lambda_1}(z_1) - f_{\lambda_1}(z_2), f_{\lambda_1}(z_2) - f_{\lambda_2}(z_2)) + Q(f_{\lambda_1}(z_2) - f_{\lambda_2}(z_2)). \end{aligned}$$

The first term in the above expression will be estimated using (4.2).

For the third term we obtain

$$\begin{aligned} Q(f_{\lambda_1}(z_2) - f_{\lambda_2}(z_2)) &\ge -\beta(\pi_y(f_{\lambda_1}(z_2) - f_{\lambda_2}(z_2))) \\ &\ge -\|\beta\| \cdot \max_{\lambda\in C}\left\|\frac{\partial \pi_y f_\lambda}{\partial \lambda}(z_2)\right\|^2 \cdot (\lambda_1 - \lambda_2)^2 \\ &\ge -\|\beta\| \max_{\lambda\in C, z\in N}\left\|\frac{\partial \pi_y f_\lambda}{\partial \lambda}(z)\right\|^2 \cdot \Gamma^2\|z_1 - z_2\|^2 = -L\Gamma^2\|z_1-z_2\|^2. \end{aligned}$$

Finally, for the second term we have

$$\begin{aligned} & |B(f_{\lambda_1}(z_1) - f_{\lambda_1}(z_2), f_{\lambda_1}(z_2) - f_{\lambda_2}(z_2))| \\ \le {} & \max_{\lambda\in C, z\in N}\left(\sum_i |a_i| \left\|\frac{\partial \pi_{z_i} f_\lambda}{\partial z}(z)\right\| \cdot \left\|\frac{\partial \pi_{z_i} f_\lambda}{\partial \lambda}(z)\right\|\right) \cdot \Gamma\|z_1 - z_2\|^2. \end{aligned}$$

From the above computations and (4.3)–(4.4) we obtain the following:

$$Q(f_{\lambda_1}(z_1) - f_{\lambda_2}(z_2)) - (1+\epsilon)Q(z_1 - z_2) \geq \left(A - 2M\Gamma - L\Gamma^2\right)\|z_1 - z_2\|^2.$$

For Γ and δ, as in (4.5) and (4.6), it is proved in [22, Lemma 23] that, for $\lambda_1, \lambda_2 \in C$, $\lambda_1 \neq \lambda_2$, and $z_i \in W^s_N(p_{\lambda_i}, f_{\lambda_i})$ for $i = 1, 2$ the following holds:

$$\delta Q(z_1 - z_2) - (\lambda_1 - \lambda_2)^2 < 0.$$

Hence $W^s_N(p_\lambda, f_\lambda)$ for $\lambda \in C$ is vertical disk in $C \times N$ for the quadratic form $\tilde{Q}(\lambda, z) = \delta Q(z) - \lambda^2$. ∎

Comments.

- Since $\tilde{Q}(x, y, \lambda) = \delta\alpha(x) - \delta\beta(y) - \lambda^2$, due to the negative sign in front of λ^2 it follows that when trying to represent the stable manifold as the vertical disk in $C \times N$, we must treat the parameter as a "stable" direction in an h-set.
- For the unstable manifold we have to take the inverse map and we obtain different δ. Since taking the inverse involves changing the sign of Q, we end up with the following quadratic form:

$$\tilde{Q}(x, y, \lambda) = \delta\alpha(x) + \lambda^2 - \delta\beta(y).$$

  Looking at the sign in front of λ^2, we see that λ appears as an "unstable" direction in $C \times N$.

5. A toy example.

In this section we show how to construct the chain of covering relations (4.1) discussed in the first part of section 4 for a special model map with a quadratic tangency which unfolds generically. Our intention is that the reader may see and appreciate some details of the method, which are later hardly visible when we report on the computer assisted proofs for the Hénon map and the forced pendulum in sections 6 and 7, respectively.

We define a map $f : \mathbb{R}^2 \to \mathbb{R}^2$ depending on the parameter a as follows:

- $(0, 0)$ is a hyperbolic fixed point, and in a neighborhood of $(0, 0)$ the map f_a is linear,

$$f_a(x, y) = (\lambda x, \mu y),$$

  where $|\lambda| > 1$ and $|\mu| < 1$;
- in a neighborhood of the point $(1, 0)$ we have the homoclinic tangency for $a = 0$. We assume that f_a acts as follows:

$$f_a(1 + x, y) = (x^2 + y + a, 1 - x).$$

When compared with the full problem of establishing the existence of generic unfolding of homoclinic tangency for the Hénon map and the forced damped pendulum, the above model map avoids the problems related to providing the explicit estimates on the dependence of $W^{s,u}$ on the parameter, which are given in Theorem 4.1.

5.1. Chain of covering relations. Let $p = (0, 0)$; then $E^u_p = [(1, 0)]$ and $E^s_p = [(0, 1)]$. Our goal is to construct a chain of covering relations "linking" (p, E^u_p) with (p, E^s_p).

The beginning of the chain. Let us first see how the covering relations look in a neighborhood of (p, E^u_p). We use the chart (x, y, v, a), where $v \mapsto [(1, v)]$. Therefore, the map $F = (Pf_a, a)$ works as follows:

$$F(x, y, v, a) = (\lambda x, \mu y, (\mu/\lambda)v, a).$$

We define an h-set, so that (x, a) are the "unstable" directions, and (y, v) are the "stable" ones. It is easy to see that there exists a sequence of h-sets $N_i = (c_i + [-x_i, x_i]) \times [-y_i, y_i] \times [-v_i, v_i] \times [-a_i, a_i]$, with $c_0 = 0$, $c_k = 1$ and such that

$$N_0 \overset{F}{\Longrightarrow} N_1 \overset{F}{\Longrightarrow} \cdots \overset{F}{\Longrightarrow} N_k.$$

Observe that the necessary conditions are

$$\begin{aligned} c_{i+1} + [-x_{i+1}, x_{i+1}] &\subset \lambda c_i + [-|\lambda| x_i, |\lambda| x_i], \\ |\mu| y_i &< y_{i+1}, \\ |\mu/\lambda|\, v_i &< v_{i+1}, \\ a_i &> a_{i+1}. \end{aligned}$$

The end of the chain. In a neighborhood of (p, E^s_p) the "unstable" subspace is (x, w), where w corresponds to the $[(w, 1)]$. The map F works as follows:

$$F(x, y, w, a) = (\lambda x, \mu y, (\lambda/\mu)w, a).$$

It is easy to see that there exists a sequence of h-sets $M_i = (\bar{c}_i + [-\bar{x}_i, \bar{x}_i]) \times [-\bar{y}_i, \bar{y}_i] \times [-\bar{w}_i, \bar{w}_i] \times [-\bar{a}_i, \bar{a}_i]$, such that

$$\bar{c}_0 = 0, \ \bar{c}_s = 1, \qquad M_s \overset{F}{\Longrightarrow} M_{s-1} \overset{F}{\Longrightarrow} \cdots \overset{F}{\Longrightarrow} M_0.$$

Observe that the necessary conditions are

$$\begin{aligned} (\bar{c}_{i+1} + [-\bar{x}_{i+1}, \bar{x}_{i+1}]) &\subset \mu \bar{c}_i + [-|\mu| \bar{x}_i, |\mu| \bar{x}_i], \\ \bar{y}_{i+1} &> |\mu| \bar{y}_i, \\ \bar{w}_{i+1} &< |\lambda/\mu|\, \bar{w}_i, \\ \bar{a}_{i+1} &< \bar{a}_i. \end{aligned}$$

Switching from the unstable to the stable manifold. We want the covering relation $N_k \overset{F}{\Longrightarrow} M_s$, where N_k and M_s are as above.

In N_k the nominally unstable directions are (x, a), while in M_s parameterized by (x, y, w, a), where $w \mapsto [(w, 1)]$, the "unstable" direction is (x, w). We have

$$F(1 + x, y, v, a) = (x^2 + y + a, 1 - x, -(2x + v), a).$$

We would like to have the following homotopy for the covering relation:

$$G_t(1+x,y,v,a) = (a+t(x^2+y), 1-tx, -2x-tv, ta).$$

Therefore, if we want a covering relation $N_k \overset{F}{\Longrightarrow} M_s$, where $N_k = (1,0,0,0)+[-x_k,x_k]\times[-y_k,y_k]\times[-v_k,v_k]\times[-a_k,a_k]$ and $M_s = (0,1,0,0)+[-\bar{x}_s,\bar{x}_s]\times[-\bar{y}_s,\bar{y}_s]\times[-\bar{w}_s,\bar{w}_k]\times[-\bar{a}_k,\bar{a}_k]$, then we need to satisfy the following set of inequalities:

$$\begin{aligned} a_k - x_k^2 - y_k &> \bar{x}_s, \\ 2x_k - v_k &> \bar{w}_s, \\ \bar{y}_s &> x_k, \\ \bar{a}_s &> a_k. \end{aligned}$$

It is easy to see that this set of inequalities has a solution. For example, if $a_k = \Delta < 1$, then we can choose (for some small $\epsilon > 0$)

$$\begin{aligned} x_k &= \Delta/2, \\ y_k = \bar{x}_s &= \Delta/3, \\ v_k = \bar{w}_s &= (1-\epsilon)\Delta/2, \\ \bar{y}_s &= (0.5+\epsilon)\Delta, \\ \bar{a}_s &= (1+\epsilon)\Delta. \end{aligned}$$

Observe that the expanding direction x is stretched in the w-direction and the a-direction is stretched across the x-direction (in the target set).

It is clear that we can easily build the desired chain of covering relation of the form

$$N_0 \overset{F}{\Longrightarrow} N_1 \overset{F}{\Longrightarrow} \cdots \overset{F}{\Longrightarrow} N_k \overset{F}{\Longrightarrow} M_s \overset{F}{\Longrightarrow} M_{s-1} \overset{F}{\Longrightarrow} \cdots \overset{F}{\Longrightarrow} M_0.$$

5.2. Cone conditions. It turns out that the cone conditions at the beginning and the end of the chain (4.1) are relatively easy to satisfy in the situation when the dynamics is linear (there is no parameter dependence) in a neighborhood of the hyperbolic fixed point; otherwise the issue becomes delicate (see Theorem 4.1 in section 4.1).

As a rule in this subsection the coordinate order for h-sets N, M will be such that the nominally unstable coordinates are always written first.

At the beginning of the chain. For covering relations $N_i \overset{F}{\Longrightarrow} N_{i+1}$ the expanding directions are (x,a). Let N_i be an h-set with Q_i-cones given by

$$Q_{N_i}(x,a,y,v) = \alpha_i x^2 + \beta_i a^2 - \gamma_i y^2 - \delta_i v^2.$$

The map F is linear for $N_i \overset{F}{\Longrightarrow} N_{i+1}$; therefore, it is enough to check whether

$$Q_{N_{i+1}}(F(x,a,y,v)) > Q_{N_i}(x,a,y,v).$$

We have

$$\begin{aligned} & Q_{N_{i+1}}(F(x,a,y,v)) - Q_{N_i}(x,a,y,v) \\ &= \alpha_{i+1}\lambda^2 x^2 + \beta_{i+1}a^2 - \gamma_{i+1}\mu^2 y^2 - (\mu/\lambda)^2\delta_{i+1}v^2 \\ &\quad - (\alpha_i x^2 + \beta_i a^2 - \gamma_i y^2 - \delta_i v^2) \\ &= (\alpha_{i+1}\lambda^2 - \alpha_i)x^2 + (\beta_{i+1} - \beta_i)a^2 + (\gamma_i - \mu^2\gamma_{i+1})y^2 + (\delta_i - (\mu/\lambda)^2\delta_{i+1}). \end{aligned}$$

Hence we will have cone conditions satisfied when, for example, $\alpha_{i+1} = \alpha_i$, $\gamma_{i+1} = \gamma_i$, $\delta_{i+1} = \delta_i$. The only strict requirement is

$$\beta_{i+1} > \beta_i.$$

At the end of the chain. In this case, the verification of the cone condition goes through easily, as in the previous case. For covering relations $M_i \overset{F}{\Longrightarrow} M_{i-1}$, the unstable directions are (x, w). We set

$$Q_{M_i}(x,w,y,a) = A_i x^2 + B_i w^2 - C_i y^2 - D_i a^2.$$

As above, it is enough to check whether

$$Q_{M_{i-1}}(F(x,w,y,a)) > Q_{M_i}(x,w,y,a).$$

We have

$$\begin{aligned} & Q_{M_{i-1}}(F(x,w,y,a)) - Q_{M_i}(x,w,y,a) \\ &\quad = (A_{i-1}\lambda^2 - A_i)x^2 + (B_{i-1}(\lambda/\mu)^2 - 1B_i)w^2 \\ &\qquad + (C_{i-1} - C_i\mu^2)y^2 + (D_{i-1} - D_i)a^2. \end{aligned}$$

We see that we need to have

$$D_{i-1} > D_i.$$

For the remaining coefficients we can set

$$A_i = A_{i-1}, B_{i-1} = B_i, C_{i-1} = C_i.$$

Switching from the unstable to the stable manifold. Consider the covering relation $N_k \overset{F}{\Longrightarrow} M_s$. This time we are in the nonlinear regime. We use on the set N_k the coordinates (x, a, y, v) and on the set M_s the coordinates (x, w, y, a).

This means that in these coordinates (we remove the shifts of the origin of the coordinate frame to $(1, 0, 0, 0)$ and $(0, 0, 1, 0)$ for N_k and M_s, respectively)

$$F(x,a,y,v) = (x^2 + y + a, -2x - v, -x, a).$$

We set

$$\begin{aligned} Q_N(x,a,y,v) &= \alpha x^2 + \beta a^2 - \gamma y^2 - \delta v^2, \\ Q_M(x,w,y,a) &= Ax^2 + Bw^2 - Cy^2 - Da^2. \end{aligned}$$

We have

$$DF(x,a,y,v) = \begin{bmatrix} 2x & 1 & 1 & 0 \\ -2 & 0 & 0 & -1 \\ -1 & 0 & 0 & 0 \\ 0 & 1 & 0 & 0 \end{bmatrix}.$$

After some computations we obtain

$$\tilde{Q} = (DF)^T Q_M DF - Q_N = \begin{bmatrix} 4Ax^2 + (4B - C - \alpha) & 2Ax & 2Ax & 2B \\ 2Ax & A - D - \beta & A & 0 \\ 2Ax & A & A + \gamma & 0 \\ 2B & 0 & 0 & B + \delta \end{bmatrix}.$$

We are interested in whether $\tilde{Q}$ is positive definite. Observe that since the positive definiteness is an open condition, we will show that $\tilde{Q}$ is positive definite for $x = 0$, and then we will know that the same holds for $|x|$ small.

After we set $x = 0$ we obtain

$$\tilde{Q} = \begin{bmatrix} 4B - C - \alpha & 0 & 0 & 2B \\ 0 & A - D - \beta & A & 0 \\ 0 & A & A + \gamma & 0 \\ 2B & 0 & 0 & B + \delta \end{bmatrix}.$$

It is easy to see that after rearrangement of the coordinates the question is reduced to the positive definiteness of the following two matrices:

$$\tilde{Q}_1 = \begin{bmatrix} 4B - C - \alpha & 2B \\ 2B & B + \delta \end{bmatrix}, \quad \tilde{Q}_2 = \begin{bmatrix} A - D - \beta & A \\ A & A + \gamma \end{bmatrix}.$$

For example, we can set $A = B = C = 1$ and $D = \frac{1}{2}$; then we obtain

$$\tilde{Q}_1 = \begin{bmatrix} 3 - \alpha & 2 \\ 2 & 1 + \delta \end{bmatrix}, \quad \tilde{Q}_2 = \begin{bmatrix} 1/2 - \beta & 1 \\ 1 & 1 + \gamma \end{bmatrix}.$$

It is now easy to see that we get what we want when we set

$$\alpha = 1, \quad \delta > 1,$$
$$\beta = 1/4, \quad \gamma > 3.$$

Summarizing, we obtained

$$Q_N(x,a,y,v) = x^2 + a^2/4 - 4y^2 - 2v^2,$$
$$Q_M(x,w,y,a) = x^2 + w^2 - y^2 - a^2/2.$$

6. Application to the Hénon map. In this section we will show that the method introduced in the previous sections can be successfully applied to a specific system. Let us consider the Hénon map [11]

$$H_{a,b}(x,y) = (a - x^2 + by, x). \tag{6.1}$$

The following theorems have been proven in [2].

Theorem 6.1 (see [2, Theorem 1.1]). *There exists an open neighborhood B of parameter value $b = 0.3$ such that for each parameter $b \in B$ there exists a parameter value*

$$a \in [1.392419807915, 1.392419807931]$$

such that the Hénon map has a quadratic tangency unfolding generically for the fixed point

$$x_{a,b} = y_{a,b} = -\frac{1}{2}\left(b - \sqrt{(b-1)^2 + 4a} - 1\right).$$

Theorem 6.2 (see [2, Theorem 1.2]). *There exists an open neighborhood B of parameter value $b = -0.3$ such that for each parameter $b \in B$ there exists a parameter value*

$$a \in [1.314527109319, 1.314527109334] \tag{6.2}$$

such that the Hénon map has a quadratic tangency unfolding generically for the fixed point

$$x_{a,b} = y_{a,b} = \frac{1}{2}\left(b - \sqrt{(b-1)^2 + 4a} - 1\right).$$

The numerical evidence of the existence of a homoclinic tangency for some parameter values $(a,b) \approx (1.3145271093265, -0.3)$ is shown in Figure 2; see also [2, Figure 1.1].

The main motivation for us to study the existence of homoclinic tangencies for the Hénon map was to verify if our method could work in this relatively easy example.

Denote by

$$a_0 = 1.3145271093265$$

a center of the interval (6.2). The aim of this section is to prove the following theorem.

Theorem 6.3. *There exists an open neighborhood B of the parameter value $b = -0.3$ such that for each $b \in B$ there is a parameter $a \in a_0 + [-10^{-5}, 10^{-5}]$ such that the Hénon map (6.1) $H_{a,b}$ has a quadratic homoclinic tangency unfolding generically for the fixed point*

$$x_{a,b} = y_{a,b} = \frac{1}{2}\left(b - \sqrt{(b-1)^2 + 4a} - 1\right) \approx -1.9679632427827796. \tag{6.3}$$

The authors in [2] report relatively long computational time (approximately 100 minutes) for the computer assisted proof of [2, Thm.1.2]. It turns out that using our method the verification of necessary inequalities in the computer assisted proof of Theorem 6.3 has been completed in 0.2 second on the Intel Xeon 5160, 3GHz processor. This very good efficiency allowed us to apply the method to a map coming from an ODE—a suitable Poincaré map in the forced damped pendulum. The details will be given in the next section.

A computer assisted proof of Theorem 6.3 will be presented in the following subsections in which we verify the following:

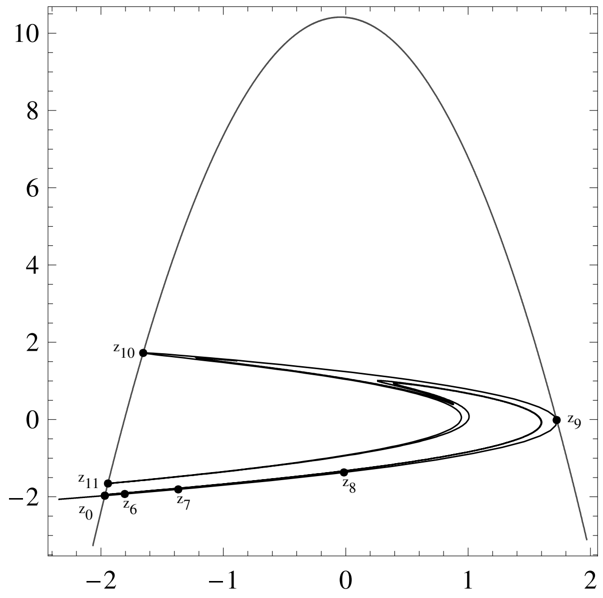

Figure 2. *Parts of the unstable and stable manifolds of the Hénon map at the fixed point for* $b = -0.3$ *and* $a = a_0 = 1.3145271093265$.

- the existence of a heteroclinic chain of covering relations for PH,
- the cone conditions along the above-mentioned heteroclinic chain,
- the cone conditions at the beginning and at the end of the chain which allow us to parameterize the center-unstable and center-stable manifolds as a horizontal or vertical disc, respectively, in proper h-sets.

6.1. The existence of a heteroclinic chain of covering relations for PH. In Theorem 6.3 we chose the center of the interval (6.2) $a_0 = 1.3145271093265$ as a good candidate for the homoclinic tangency parameter corresponding to $b_0 = -0.3$.

In order to define the sets which will appear in the heteroclinic chain, we need to set a local chart for the manifold $P\mathbb{R}^2$. It turns out that it is enough for our purpose to use the parameterization

$$\psi : \mathbb{R}^2 \times (0, \pi) \ni (x, y, t) \mapsto (x, y, [(\cos(t), \sin(t))]) \in P\mathbb{R}^2. \tag{6.4}$$

This parameterization excludes one point on the manifold, but through our computations this point does not appear either as an argument or as a value of PH_a. All the sets will be expressed using coordinates (x, y, t, a).

Put

$$PH(x, y, t, a) = \left((\psi^{-1} \circ PH_{a,b_0} \circ \psi)(x, y, t), a\right). \tag{6.5}$$

In what follows by π_t we will denote a projection onto the tangent coordinate; i.e., for $[u]$ such that $u_2 > 0$ we define

$$\pi_t(x, y, [u]) = \frac{u}{\|u\|}.$$

With some abuse of notation we will use the same symbols for the projections

$$\pi_t(x,y,[u],a) = \frac{u}{\|u\|} \quad \text{or} \quad \pi_t(x,y,t,a) = (\cos(t),\sin(t)),$$

but it is clear from the list of arguments which projection has to be used. In each case the value of π_t is a vector.

To simplify the notation we will use $z_0 = (x_0,y_0) = (x_{a_0,b_0}, y_{a_0,b_0})$ as defined in (6.3). Since we will always have the fixed value of the parameter $b_0 = -0.3$, we will write H_a instead of H_{a,b_0} in what follows. Let u_0 and s_0 be normalized with respect to the Euclidean norm eigenvectors of $DH_{a_0}(z_0)$ given explicitly by

$$\begin{aligned} u_0 &= \frac{(-x_0+\sqrt{x_0^2+b_0},1)}{\left\|(-x_0+\sqrt{x_0^2+b_0},1)\right\|} \approx (0.9680131177714217873, 0.250899589123719882),\\ s_0 &= \frac{(-x_0-\sqrt{x_0^2+b_0},1)}{\left\|(-x_0-\sqrt{x_0^2+b_0},1)\right\|} \approx -(0.077523077959933337433, 0.996990557820693689), \end{aligned} \tag{6.6}$$

and let $M = [u_0^T, s_0^T]$ be a matrix of eigenvectors. Put

$$z_1 = z_0 + 0.0001993152279412426 u_0 + 2.50404 \cdot 10^{-11} s_0.$$

The above point has been chosen as a good approximation of the homoclinic tangency point for H_{a_0}. Namely, we have

$$\begin{aligned} \|H_{a_0}^{-1}(z_1) - z_0\| &\leq 5.2 \cdot 10^{-5},\\ \|H_{a_0}^{14}(z_1) - z_0\| &\leq 1.2 \cdot 10^{-5},\\ M^{-1}\left(\pi_t\left(PH_{a_0}^{14}(z_1,[u_0])\right)\right) &\approx (-4.71 \cdot 10^{-7}, 0.999999847). \end{aligned} \tag{6.7}$$

We see that the unstable direction u_0 at z_1 is mapped under the 14th iterate of H_{a_0} very close to the stable direction s_0 at the point $H_{a_0}^{14}(z_1)$. Let us underline that to get the estimation (6.7) we need to compute $DH_{a_0}^{14}$ with at least *long double* precision of the floating point arithmetics.

The points on the trajectory of z_1 will be the centers of the sets which appear in the computer assisted proof. Put

$$\begin{aligned} c_0 &= (\psi^{-1}(z_0,u_0),a_0),\\ c_1 &= (\psi^{-1}(z_1,u_0),a_0),\\ c_{i+1} &= PH^i(c_1) \quad \text{for } i=1,\dots,13,\\ c_{15} &= (\psi^{-1}(z_0,s_0),a_0). \end{aligned}$$

For further use we set also

$$\begin{aligned} z_{i+1} &= H_{a_0}^i(z_1) \quad \text{for } 1=1,\dots,13,\\ z_{15} &= z_0. \end{aligned}$$

Some of these points are shown in Figure 2.

Now, we have to choose approximate stable and unstable directions at c_i, $i = 0, \ldots, 15$. On each set centered at c_i, the coordinate system will be given by a matrix

$$M_i = \begin{bmatrix} (u_i)_1 & (s_i)_1 & 0 & 0 \\ (u_i)_2 & (s_i)_2 & 0 & 0 \\ 0 & 0 & 1 & 0 \\ 0 & 0 & 0 & 1 \end{bmatrix}, \tag{6.8}$$

where u_0, s_0 are given by (6.6) and u_i and s_i are computed as follows.

- Put $u_{15} = u_0$, $s_{15} = s_0$, $u_1 = u_0$, $s_1 = s_0$.
- For $i = 2, \ldots, 8$ we set

$$u_i = \pi_t(c_i), \tag{6.9}$$

$$s_i = \pi_t(PH^{-1}(z_{i+1}, \pi_t(c_{i+1})^{\perp})). \tag{6.10}$$

  From numerical simulations we get that between the points c_8 and c_9 the role of the tangent coordinate is changing from contracting to expanding. Therefore, the unstable direction propagates very well on these sets just by (6.9) for $i = 2, \ldots, 8$. For the inverse map, the unstable directions u_i become repelling. Therefore, the preimage of an orthogonal direction to u_{i+1} becomes a good enough approximation for our method of the stable direction at z_i.
- According to a good choice of the homoclinic point (6.7), the tangent coordinate at c_i becomes a good approximation of the stable direction on sets centered at $c_9, \ldots, c_{14}$. Therefore, we can set

$$\begin{aligned} s_i &= \pi_t(c_i) \quad \text{for } i = 9, \ldots, 14, \\ u_9 &= \pi_t(PH_{a_0}(z_8, [s_8])), \\ u_{i+1} &= \pi_t(PH_{a_0}(z_i, [u_i])) \quad \text{for } i = 9, \ldots, 13. \end{aligned}$$

There remains for us to set the sizes of the sets. We define the h-sets by

$$N_i = c_i + M_i \cdot (d_i \cdot [-1, 1]), \tag{6.11}$$

where the diameters d_i are listed in Table 1 and are chosen from numerical experiments. On h-sets $N_0, \ldots, N_8$ the expanding directions are u and a coordinates, while on $N_9, \ldots, N_{15}$ the expanding directions are u and t coordinates.

Let us comment briefly about the choice of the sizes of the sets presented in Table 1. For the sets $N_0, \ldots, N_8$ the tangent coordinate is chosen as a contracting direction. Therefore, the set in this direction must be large enough (here, $2 \cdot 10^{-5}$) to be able to easily verify that we have contraction on this variable. On the other hand, for the sets $N_9, \ldots, N_{15}$ we have a strong expansion on this coordinate. Therefore, the diameter of these sets on this coordinate is smaller here because it is easier to verify that the image of some walls of the previous set in the chain is outside of a small set than inside of it.

Moreover, the tangent coordinate of N_9 has to be covered by the unstable coordinate of N_8. This expansion is weak and forces decreasing of the size N_9 on the tangent coordinate.

Table 1

Diameters of the h-sets in the heteroclinic sequence for the Hénon map. The diameters in the table are scaled by the factor 10^5. On h-sets $N_0, \ldots, N_8$ the expanding directions are u and a coordinates, while on $N_9, \ldots, N_{15}$ the expanding directions are u and t coordinates.

i	$10^5 \cdot (d_i)_1$ unstable dir.	$10^5 \cdot (d_i)_2$ stable dir.	$10^5 \cdot (d_i)_3$ tangent dir.	$10^5 \cdot (d_i)_4$ parameter
0	7	1	2	$(1.01)^8$
1	1	1	2	$(1.01)^7$
2	1	1	2	$(1.01)^6$
3	1	1	2	$(1.01)^5$
4	1	1	2	$(1.01)^4$
5	1	1	2	$(1.01)^3$
6	1	1	2	$(1.01)^2$
7	1	1	2	1.01
8	1	1	2	1
9	0.5	1.25	0.25	1.01
10	0.75	1.25	0.25	$(1.01)^2$
11	1	1.25	0.25	$(1.01)^3$
12	1	1.25	0.25	$(1.01)^4$
13	1	1.25	0.25	$(1.01)^5$
14	1	1.25	0.25	$(1.01)^6$
15	1	2	0.25	$(1.01)^7$

The unstable and stable directions are comparable for almost all sets in the chain except N_0, N_9, and N_{15}. For N_0 we have a large size in the unstable direction. This is due to the fact that N_1 is at some distance from z_0. The size $7 \cdot 10^{-5}$ is necessary to reach the set N_1 from N_0.

Similar reasoning applies to N_{15}. The stable size must be large enough so that the image of N_{14} is captured in this direction.

On the set N_9 we have a change of dynamics. The unstable size of N_9 is smaller since on N_8 the parameter plays a role of expanding the direction which covers the unstable direction on N_9. Since this expansion is weak, we must decrease the size of N_9. On the other hand, the image of N_8 varies with the parameter and is larger in the stable direction of N_9. This forces us to enlarge the set N_9 a little bit in the stable direction.

Now we can state the first numerical lemma.

Lemma 6.4. *The following covering relations hold true:*

$$N_0 \overset{PH}{\Longrightarrow} N_1 \overset{PH}{\Longrightarrow} \cdots \overset{PH}{\Longrightarrow} N_{15}.$$

Proof. The assertion of the above lemma has been verified using the interval arithmetics [13] and the algorithms for verifying the existence of covering relations described in [20]. We were able to verify the necessary inequalities on each wall of N_i, $i = 0, \ldots, 15$, without any subdivision of the sets, so the computational time was less than one second. ■

6.2. The cone conditions along the heteroclinic chain. In this section we will show that the cone conditions are satisfied for the sequence of covering relations from Lemma 6.4. We have two results which give us a numerical method for verifying the cone conditions.

Lemma 6.5 (see [12, Lemma 6]). *Let (N, Q_N) and (M, Q_M) be h-sets with cones in $\mathbb{R}^n$, and let $f : N \to \mathbb{R}^n$ be $\mathcal{C}^1$ such that $N \overset{f}{\Longrightarrow} M$. Let $[Df(N)]_I$ denote the interval enclosure of the set of matrices $Df(N)$. If the interval matrix*

$$V = [Df(N)]_I^T Q_M [Df(N)]_I - Q_N$$

is positive definite, then the cone conditions are satisfied for the covering relation $N \overset{f}{\Longrightarrow} M$.

Let $A = A_c + [-1, 1] \cdot A_0$ be an interval matrix, where $A_c, A_0 \in \mathbb{R}^{n\times n}$ are real and symmetric. For $z \in \mathbb{R}^n$ by $\Delta(z)$ we will denote a diagonal matrix with z_i's at the diagonal.

Lemma 6.6 (see [16, Theorem 2]). *The interval matrix $A = A_c + [-1, 1] \cdot A_0$ is positive definite iff for each sequence $z \in \{-1, 1\}^n$ the matrix*

$$A_z = A_c - \Delta(z)A_0\Delta(z)$$

is positive definite.

In light of the above lemma, to verify that a symmetric interval matrix is positive definite, it is enough to verify if 2^{n-1} real matrices A_z are positive definite.

In order to verify the cone conditions, we have to define quadratic forms on the sets N_i, $i = 0, \ldots, 15$. Denote by

$$\lambda = 3.858169402, \quad \mu = 0.07775708341 \tag{6.12}$$

approximate eigenvalues of DH_{a_0} at z_0. Recall that by $\Delta(p_1, \ldots, p_n)$ we denote a diagonal matrix with p_i's at the diagonal. For $i = 0, \ldots, 15$ we define the quadratic form on the h-set N_i by

$$Q_i = \Delta\left((p_i)_1, (p_i)_2, (p_i)_3, (p_i)_4\right),$$

where the coefficients are listed in Table 2. The quadratic forms Q_i are defined in the coordinate systems given by matrices M_i (6.8) used to define the h-sets N_i, $i = 0, \ldots, 15$. These matrices have normalized columns. In these coordinates the sets are given by $N_i = [(d_i)_1, \ldots, (d_i)_4] \cdot [-1, 1]$, $i = 0, \ldots, 15$; see (6.11) and Table 1.

Let us comment briefly on the choice of these coefficients. Assume that we would like to verify the cone conditions for the covering relation $N \overset{f}{\Longrightarrow} M$. Assume that f is linear and in some coordinate systems on N and M it is given by $f = \Delta(\lambda_1, \ldots, \lambda_k)$. In the general case, we usually have $Df(N)$ close to a diagonal matrix, but the arguments apply. Assume also that the quadratic forms on both sets N and M are diagonal and given by

$$Q_N = \Delta(\alpha_1^N, \ldots, \alpha_k^N),$$
$$Q_M = \Delta(\alpha_1^M, \ldots, \alpha_k^M).$$

According to Lemma 6.5, the cone conditions will be satisfied if the interval matrix

$$V = [Df(N)]_I^T \cdot Q_M \cdot [Df(N)]_I - Q_N = \Delta(\lambda_1^2\alpha_1^M - \alpha_1^N, \ldots, \lambda_k^2\alpha_k^M - \alpha_k^N)$$

is positive definite. We see that if $|\alpha_i^{N,M}| = 1$ and some $|\lambda_i| \gg 1$, then the corresponding coefficient in the matrix V becomes very large, while for $|\lambda_j| \ll 1$ the corresponding coefficient

Table 2

Coefficients of the quadratic forms on the sets $N_0, \dots, N_{15}$, where $\lambda = 3.858169402$, $\mu = 0.07775708341$ are approximate eigenvalues of $DH_{a_0}(z_0)$.

i	$(p_i)_1$ unstable dir.	$(p_i)_2$ stable dir.	$(p_i)_3$ tangent dir.	$(p_i)_4$ parameter
0	$3/\lambda^2$	$-\mu^2$	$-(\mu/\lambda)^2$	$2(1.5)^{-8}$
1	$1/\lambda^2$	-0.1	-0.5	$2(1.5)^{-7}$
2	$1/\lambda^2$	-0.1	-1	$2(1.5)^{-6}$
3	$1/\lambda^2$	-0.1	-1	$2(1.5)^{-5}$
4	$1/\lambda^2$	-0.1	-1	$2(1.5)^{-4}$
5	$1/\lambda^2$	-0.1	-1	$2(1.5)^{-3}$
6	$1/\lambda^2$	-0.1	-1	$2(1.5)^{-2}$
7	$1/\lambda^2$	-0.1	-1	$2(1.5)^{-1}$
8	$0.5/\lambda^2$	-1	-1	2
9	$100/\lambda^2$	-0.1	$100(\mu/\lambda)^2$	-2
10	$40/\lambda^2$	-0.1	$(\mu/\lambda)^2$	$-2(1.5)^{-1}$
11	$10/\lambda^2$	-0.1	$(\mu/\lambda)^2$	$-2(1.5)^{-2}$
12	$1/\lambda^2$	-0.1	$(\mu/\lambda)^2$	$-2(1.5)^{-3}$
13	$1/\lambda^2$	-0.1	$(\mu/\lambda)^2$	$-2(1.5)^{-4}$
14	$1/\lambda^2$	-0.1	$(\mu/\lambda)^2$	$-2(1.5)^{-5}$
15	$0.3/\lambda^2$	-0.1	$(\mu/\lambda)^2$	$-2(1.5)^{-6}$

in V is close to 1. In the general (nonlinear) case we have some nonzero intervals off the diagonal of V. Therefore, from the computational point of view, it is better to make the matrix V somehow uniform, i.e., such that the coefficients on the diagonal are of the same magnitude. This can be achieved by setting coefficients $\alpha_i \approx \lambda_i^{-2}$ for these i such that $|\lambda_i| \gg 1$.

This can be seen in the first column of Table 2 and the second part of the third column.

The coefficients for N_9 are chosen so as to be able to switch from the unstable to the stable manifold.

Notice also a different choice of the coefficients for the quadratic form Q_0 in N_0. The reason is that we have to prove that the center-unstable manifold at the fixed point c_0 is a horizontal disk in N_0 satisfying the cone conditions. Therefore, we need to apply the method described in Theorem 4.1 to the inverse of PH. In this case, the coefficients in the second and the third columns correspond to expanding directions with approximate eigenvalues $1/\mu$ and λ/μ, both greater than 1.

We have the following lemma.

Lemma 6.7. *The cone conditions are satisfied for the sequence of covering relations*

$$N_0 \overset{PH}{\Longrightarrow} N_1 \overset{PH}{\Longrightarrow} \cdots \overset{PH}{\Longrightarrow} N_{15}.$$

Proof. Observe that verification of the cone conditions for these covering relations requires computation of the DPH, which involves the second order derivatives of H. In the computer assisted proof we computed an enclosure for $DPH(N_i)$, $i = 0, 1 \dots, 14$, using whole N_i without subdivision as an initial condition of the routine which computes DPH. Then we applied Lemma 6.5 and Lemma 6.6 to prove that the cone conditions are satisfied. The C++

program which verifies the assertion executes within less than one second on a laptop-type computer. ∎

6.3. Parameterization of center-unstable and center-stable manifolds at c_0 and c_{15}, respectively. In this section we will use the method described in Theorem 4.1 in order to parameterize the center-unstable and center-stable manifolds as horizontal and vertical discs satisfying the cone conditions in N_0 and N_{15}, respectively. This, together with Lemma 6.4 and Lemma 6.7, will give us a proof of Theorem 6.3.

Put

$$\widetilde{N_0} = (z_0, [u_0]) + \widetilde{M} \cdot ((d_0)_1, (d_0)_2, (d_0)_3)\,,$$
$$\widetilde{N_{15}} = (z_0, [s_0]) + \widetilde{M} \cdot ((d_{15})_1, (d_{15})_2, (d_{15})_3)\,,$$

where $\widetilde{M}$ is a 3×3 minor of the matrix $M_{15} = M_0$ (see (6.8)) after removing the last column and the last row. The coefficients $(d_i)_j$ are listed in Table 1. Geometrically, these sets are just projections onto (x, y, t) coordinates of N_0 and N_{15}, respectively.

The set $\widetilde{N_{15}}$ is a three-dimensional h-set with two expanding directions (corresponding to eigenvalues λ and $\frac{\lambda}{\mu}$) and one nominally stable direction (corresponding to the eigenvalue μ), where λ, μ are eigenvalues of $DH_{a_0}(z_0)$; see (6.12).

On the set $\widetilde{N_0}$ we will compute the inverse map of PH_a so that the roles of nominally stable and nominally unstable directions interchange. Hence, the set $\widetilde{N_0}$ has two nominally unstable directions (with eigenvalues μ^{-1} and λ/μ) and one nominally stable direction (with eigenvalue λ^{-1}).

On both sets we set quadratic forms defining the cones to be equal to

$$\widetilde{Q_0} = -\Delta\left((p_0)_1, (p_0)_2, (p_0)_3\right), \tag{6.13}$$
$$\widetilde{Q_{15}} = \Delta\left((p_{15})_1, (p_{15})_2, (p_{15})_3\right), \tag{6.14}$$

where the coefficients are listed in Table 2.

Lemma 6.8. *The center-stable manifold of PH at c_{15} can be parameterized as a vertical disk in N_{15} satisfying the cone conditions with respect to the quadratic form Q_{15}.*

Proof. We use Theorem 4.1. Let π_a denote a projection onto the parameter coordinate. With computer assistance we verified that for $a \in \pi_a(N_{15})$ it holds that

$$\widetilde{N_{15}} \overset{PH_a}{\Longrightarrow} \widetilde{N_{15}},$$

and the cone conditions are satisfied with the quadratic form $\widetilde{Q_{15}}$. Hence, the first assumption of Theorem 4.1 is fulfilled.

Then we computed the constants A, M, L which appear in assumptions 2–3 of Theorem 4.1 and we obtained

$$A \geq 0.099394300936541294,$$
$$M \leq 0.084042214456891598,$$
$$L \leq 0.0070394636406844067.$$

Hence constant Γ from assumption 4 of Theorem 4.1 can be chosen to be equal to $\Gamma = 0.57737423322563175$. With this Γ the coefficient δ defined in (4.6) is equal to

$$\delta = \frac{\Gamma^2}{\|\alpha\|} \leq 16.54078540195168,$$

where α appears in the decomposition of the quadratic form $\widetilde{Q_{15}}(x, y, t) = \alpha(x, t) - \beta(y)$ and $\|\alpha\| = \max\left\{0.3/\lambda^2, (\mu/\lambda)^2\right\} = 0.3/\lambda^2$; see Table 2.

From Theorem 4.1 it follows that the center-stable manifold of PH at c_{15} can be parameterized as a vertical disk in N_{15} satisfying the cone conditions with respect to the quadratic form

$$\overline{Q_{15}}(x, y, t, a) = \delta\widetilde{Q_{15}}(x, y, z) - a^2.$$

Recall that by Q_{15} we denote the quadratic form on N_{15}. To finish the proof let us observe that

$$Q_{15}(x, y, t, a) = \widetilde{Q_{15}}(x, y, t) - 2(1.5)^{-6}a^2;$$

see (6.14) and Table 2. Moreover, we have $2(1.5)^{-6}\delta > 1$. This shows that

$$\delta Q_{15}(x, y, t, a) = \delta\left(\widetilde{Q_{15}}(x, y, t) - 2(1.5)^{-6}a^2\right) < \overline{Q_{15}}(x, y, t, a).$$

Therefore, the center-stable manifold of PH at c_{15} is a vertical disk in N_{15} satisfying the cone condition for the quadratic form Q_{15}. ■

We have a similar lemma about the parameterization of the center-unstable manifold of PH at c_0 as a horizontal disk in N_0.

Lemma 6.9. *The center-unstable manifold of PH at c_0 can be parameterized as a horizontal disk in N_0 satisfying the cone conditions with respect to the quadratic form Q_0.*

Proof. We will proceed as in Lemma 6.8 but for the map PH^{-1}. With computer assistance we verified that for $a \in \pi_a(N_0)$ it holds that

$$\widetilde{N_0} \overset{PH_a^{-1}}{\Longrightarrow} \widetilde{N_0}$$

and the cone conditions are satisfied. We computed the constants which appear in (4.5)–(4.6), and we got

$$\begin{aligned}
A &\geq 0.1877584261322994,\\
M &\leq 0.2795983187542756,\\
L &\leq 0.015049353557694945,\\
\Gamma &= 0.33278415598142302,\\
\delta &\leq 18.316620936531205.
\end{aligned}$$

Hence, the center-stable manifold for PH^{-1} at c_0 is a vertical disk in N_0 satisfying the cone condition for the quadratic form

$$\overline{Q_0(x, y, t, a)} = \delta\widetilde{Q_0}(x, y, t) - a^2.$$

From (6.13) and Table 2 we have

$$Q_0(x,y,t,a) = -\widetilde{Q_0}(x,y,t,a) + 2(1.5)^{-8}a^2.$$

Since $2(1.5)^{-8}\delta > 1$, we have

$$-\delta Q_0(x,y,t,a) = \delta\left(\widetilde{Q_0}(x,y,t,a) - 2(1.5)^{-8}a^2\right) < \overline{Q_0(x,y,t,a)},$$

and the center-stable manifold of PH^{-1} at c_0 can be parameterized as a vertical disk in N_0 satisfying the cone conditions with respect to the quadratic form $-Q_0$. This means that the center-unstable manifold of PH can be parameterized as a horizontal disk in N_0 satisfying the cone conditions with respect to the quadratic form Q_0. ■

Proof of Theorem 6.3. We obtain our conclusion from Lemmas 6.7, 6.8, and 6.9 combined with the discussion of the strategy of the proof in the first part of section 4. ■

7. Application to the forced damped pendulum equation.

Let us consider an equation for the forced damped pendulum motion

$$\ddot{x} + \beta\dot{x} + \sin(x) = \cos(t). \tag{7.1}$$

Equation (7.1) is a well-known example of an equation which exhibits chaotic dynamics; see [10] and references therein. In [3] it has been proven (a computer assisted proof) that for the parameter $\beta = 0.1$ the 2π-time map is semiconjugated to the full shift on three symbols on some compact invariant set.

Equation (7.1) defines a flow on $\mathbb{R}^2 \times S^1$, where S^1 is a unit circle. Let us define the Poincaré map $T_\beta\colon \mathbb{R}^2 \to \mathbb{R}^2$ by

$$T_\beta(x,\dot{x}) = \left(x(2\pi), \dot{x}(2\pi)\right), \tag{7.2}$$

where $x(t)$ is a solution of (7.1) with the parameter β.

The aim of this section is to prove the following theorem.

Theorem 7.1. *For all parameter values*

$$\beta \in \mathcal{B} = 0.247133729485 + [-1,1]\cdot 1.2\cdot 10^{-10}$$

there exists a hyperbolic fixed point for T_β corresponding to a 2π periodic solution of (7.1). *Moreover, there exists a parameter value $\beta \in \mathcal{B}$ such that the map T_β has a quadratic homoclinic tangency unfolding generically for that fixed point.*

The proof of Theorem 7.1 uses the same method as for the Hénon map case. Since all the details have been discussed in section 6, we will give here only the definition of the sets and quadratic forms, and we will state the numerical lemmas.

The main difference between the Hénon map case and that of the forced damped pendulum equation is how we compute derivatives of a map up to the second order, required in the proof. Since the Hénon map is given explicitly, these derivatives can be computed by hand or using the Automatic Differentiation tools [9]. For the forced damped pendulum equation we used the C^r-Lohner algorithm presented in [21]. This algorithm allows us to efficiently integrate the variational equations for ODEs and compute partial derivatives of Poincaré maps.

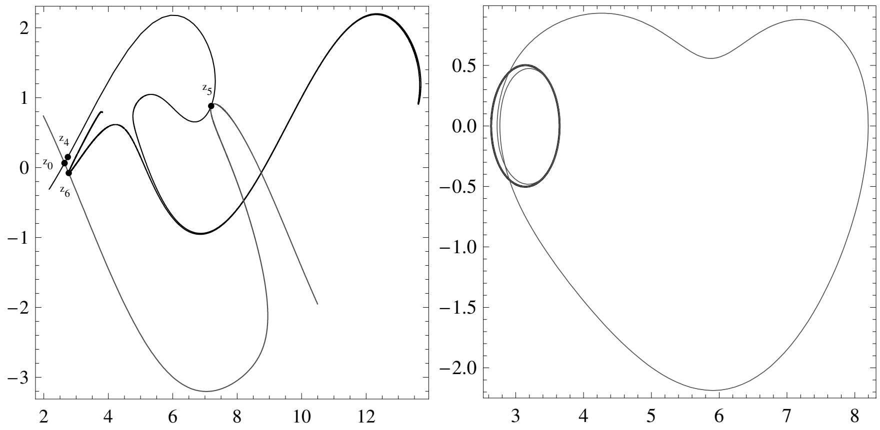

Figure 3. *Left: Parts of the unstable and stable manifolds of a fixed point of T_β for $\beta = 0.247133729485$. Right: Periodic orbit and a homoclinic orbit to the periodic orbit for (7.1) projected onto $(x, \dot{x})$ coordinates. This homoclinic orbit corresponds to the quadratic tangency of invariant manifolds. The left picture suggests also the existence of transversal homoclinic points.*

7.1. Heteroclinic chain of covering relations. Let $PT_\beta : P\mathbb{R}^2 \to P\mathbb{R}^2$ denote the map induced by T_β on the projective bundle, and let ψ be a local parameterization of the space $P\mathbb{R}^2$ as defined in (6.4). Let

$$PT : P\mathbb{R}^2 \times \mathbb{R} \ni (x, \dot{x}, t, \beta) = \big((\psi^{-1} \circ PT_\beta \circ \psi)(x, \dot{x}, t), \beta\big) \in P\mathbb{R}^2 \times \mathbb{R}.$$

Let

$$\beta_0 = 0.247133729485,$$
$$z_0 = (2.6410109874338904, 0.063471204982120187),$$
(7.3) $$u_0 = (0.76818278871270265, 0.64023058590290362),$$
(7.4) $$s_0 = (0.67655372773981033, -0.73639327365298942),$$
(7.5) $$\lambda = 211.83022271012155,$$
(7.6) $$\mu = 0.00099918347695168025.$$

From numerical experiments we got that z_0 (see Figure 3) is an approximate fixed point for T_{β_0} with approximate eigenvalues λ, μ and approximate eigenvectors u_0, s_0, respectively. This point has been found by the standard Newton method.

Let us denote

$$\begin{array}{rclrcl} & & & c_0 & = & \psi^{-1}((z_0, u_0), \beta_0), \\ z_1 & = & z_0 + 1.41442890240556 \cdot 10^{-8} u_0, & c_1 & = & \psi^{-1}((z_1, u_0), \beta_0), \\ z_i & = & T_{\beta_0}(z_{i-1}) \text{ for } i = 2,3,4,5, & c_i & = & PT(c_{i-1}) \text{ for } i = 2,3,4,5, \\ z_8 & = & z_0 + 19.0992395815 \cdot 10^{-8} s_0, & c_8 & = & \psi^{-1}((z_8, s_0), \beta_0), \\ z_i & = & T^{-1}_{\beta_0}(z_{i+1}) \text{ for } i = 7,6, & c_i & = & PT^{-1}(c_{i-1}) \text{ for } i = 7,6, \\ z_9 & = & z_0, & c_9 & = & \psi^{-1}((z_0, s_0), \beta_0). \end{array}$$

Some of these points are shown in Figure 3. The points z_1 and z_8 are chosen close to a heteroclinic trajectory for T_{β_0}. Numerical simulation shows that

$$PT^{-1}(c_6) - c_5 \approx (3.42 \cdot 10^{-12}, 6.34 \cdot 10^{-12}, -2.32 \cdot 10^{-8}, 0). \tag{7.7}$$

In fact, we observe that between c_5 and c_6 the role of the tangent direction changes and at c_6 it becomes repelling.

The reason for which we define two points z_1 and z_8 and compute their forward and backward trajectories, respectively, is due to the numerical problems with forward propagation of the tangent coordinate at z_6, z_7, even in simulation only. Recall that the tangent coordinate t becomes strongly repelling at z_6 and z_7 with eigenvalue of the order 10^5. Therefore, it is easier to propagate the preimage of the stable direction at z_8 which is attracting at z_7 and z_6 for the inverse map.

Approximate estimation (7.7) shows us that the points c_i, $i = 1, \ldots, 8$, are close to the possible existing heteroclinic trajectory for PT.

Now we will define the coordinate systems of the h-sets centered at c_i's. Let M_i be the matrix of the coordinate system of the set centered at c_i. We assume that M_i has the form (6.8). These matrices are computed as follows:

- Put $u_9 = u_0,\ u_1 = u_0,\ u_8 = u_0$ and $s_9 = s_0,\ s_1 = s_0,\ s_8 = s_0$, where u_0, s_0 are defined by (7.3)–(7.4).
- For $i = 2, 3, 4, 5$ we set

$$\begin{aligned} u_i &= \pi_t(c_i),\\ s_i &= \pi_t(PT^{-1}_{\beta_0}(z_{i+1}, \pi_t(c_{i+1})^\perp)), \quad i = 2,3,4,\\ s_5 &= u_5^\perp. \end{aligned}$$

- For $i = 6, 7$ we set

$$\begin{aligned} s_i &= \pi_t(c_i),\\ u_i &= \pi_t\left(PT_{\beta_0}\left(T^{-1}(z_i), \pi_t\left(PT^{-1}_{\beta_0}(z_i, s_i)\right)^\perp\right)\right). \end{aligned}$$

As in the case of the Hénon map, the h-sets $N_0, \ldots, N_9$ for the map PT will be defined by formula (6.11) with matrices M_i as above and the diameters given in Table 3.

The h-sets $N_0, \ldots, N_5$ have two unstable directions given by u_i and the parameter. The h-sets $N_6, \ldots, N_9$ have two unstable directions given by u_i and the tangent coordinate.

Now, we can state the following numerical lemma.

Lemma 7.2. *The map PT is well defined and continuous on $\bigcup_{i=0}^9 N_i$. Moreover, the following covering relations hold true:*

$$N_0 \overset{PT}{\Longrightarrow} N_1 \overset{PT}{\Longrightarrow} \cdots \overset{PT}{\Longrightarrow} N_9. \tag{7.8}$$

Proof. In the computer assisted proof of the above lemma we used the C^1-Lohner algorithm [22] and the CAPD library [8] in order to integrate the variational equations for (7.1) and to compute the map PT. We used the Taylor method of the order 20 with a variable time step.

Table 3

Diameters of the h-sets in the heteroclinic sequence for the PT map. The h-sets $N_0,\dots,N_5$ have two unstable directions given by u_i and the parameter. The h-sets $N_6,\dots,N_9$ have two unstable directions given by u_i and the tangent coordinate.

i	$10^{10}\cdot(d_i)_1$ unstable dir.	$10^{10}\cdot(d_i)_2$ stable dir.	$10^{8}\cdot(d_i)_3$ tangent dir.	$10^{10}\cdot(d_i)_4$ parameter
0	5	0.2	0.26	$1.2(1.01)^5$
1	0.4	6	2	$1.2(1.01)^4$
2	0.4	6	4	$1.2(1.01)^3$
3	0.6	6	2	$1.2(1.01)^2$
4	5	2	1	$1.2(1.01)$
5	27	2	1	1.2
6	0.4	15	0.4	$1.2(1.01)$
7	0.4	8	0.4	$1.2(1.01)^2$
8	0.4	10	1.2	$1.2(1.01)^3$
9	0.4	5	0.2	$1.2(1.01)^4$

To verify the inequalities required for the covering relations we subdivided the boundary of each h-set with a grid depending on the set under consideration. The total number of boxes we used is 5546. The C++ program which verifies the existence of covering relations (7.8) executes within 18 seconds on a computer with the Intel Xeon 5160, 3GHz processor. ■

7.2. The cone conditions along the heteroclinic chain of covering relations for the map PT. Recall that for a $p\in\mathbb{R}^n$ by $\Delta(p)$ we denoted a diagonal matrix with p_i's on the diagonal.

For $i=0,\dots,9$ we define the quadratic form on the h-set N_i by

$$Q_i=\Delta\left((p_i)_1,(p_i)_2,(p_i)_3,(p_i)_4\right),$$

where the coefficients are listed in Table 4.

Let us comment on the choice of these coefficients. In the example presented in section 5 there is no dependency on the parameter; hence the cone conditions are easily achievable. In the general case this dependency has a huge influence on the choice of the parameters in quadratic forms corresponding to the parameter variable. In fact, this sometimes forces large scaling (not only by some small factor, like in the Hénon map case).

The other constraints on the coefficients are related to the parameterization of center-unstable and center-stable manifolds in the first and last sets in the heteroclinic chain of covering relations.

The main constraint, however, appears for the covering relation in the switch between manifolds. Here it is necessary to set relatively large coefficients corresponding to both unstable variables in the set after this switch and a small coefficient for the stable variable in the main phase space. This can be seen in Tables 2 and 4 for the sets N_9 and N_6, respectively. In the next sets we can use the hyperbolicity of the map to make these coefficients more uniform and to reach constraints at the beginning and at the end of the chain.

For $i=2,\dots,9$ the coordinate systems on N_i are given by the matrices M_i used to define the sets N_i, respectively.

Table 4

Coefficients of the quadratic forms on the sets $N_0, \dots, N_9$, where λ, μ are approximate eigenvalues of $DT_{\beta_0}(z_0)$ and are given in (7.5)–(7.6).

i	$(p_i)_1$ unstable dir.	$(p_i)_2$ stable dir.	$(p_i)_3$ tangent dir.	$(p_i)_4$ parameter
0	$80/\lambda^2$	$-\mu^2$	$-(\mu/\lambda)^2$	$(1.1)^{-5}$
1	$1/\lambda^2$	-0.01	-10^{-7}	$(1.1)^{-4}$
2	$1/\lambda^2$	-1	-10^{-5}	$(1.1)^{-3}$
3	$1/\lambda^2$	-1	-10^{-5}	$(1.1)^{-2}$
4	$1/\lambda^2$	-1	-10^{-5}	$(1.1)^{-1}$
5	$10/\lambda^2$	-1	-10^{-5}	3
6	$1000/\lambda^2$	-10^{-4}	$10^6(\mu/\lambda)^2$	$-(1.1)^{-1}$
7	$1/\lambda^2$	-1	$(\mu/\lambda)^2$	$-(1.1)^{-2}$
8	$1/\lambda^2$	-1	$(\mu/\lambda)^2$	$-(1.1)^{-3}$
9	$1/\lambda^2$	-1	$(\mu/\lambda)^2$	$-(1.1)^{-4}$

We have the following numerical result.

Lemma 7.3. *The cone conditions are satisfied for the sequence of covering relations*

$$N_0 \overset{PT}{\Longrightarrow} N_1 \overset{PT}{\Longrightarrow} \cdots \overset{PT}{\Longrightarrow} N_9.$$

Proof. By Lemma 6.5 it is enough to verify that for $i = 0, \dots, 8$ the interval matrix

$$V_i = [DPT(N_i)]_I^T Q_{N_{i+1}} [DPT(N_i)]_I - Q_{N_i}$$

is positive definite, where DPT is computed in the coordinate systems of N_i and N_{i+1}. Notice that to compute DPT we need second order derivatives of the map T. We used the C^2-Lohner algorithm [21] and the CAPD library [8] in order to integrate the second order variational equations for (7.1). We used the Taylor method of the order 20 and a variable time step. No subdivision of the sets N_i was necessary; i.e., whole sets N_i were used as an initial condition for the routine which computes DPT. The C++ program which verifies the cone conditions from this lemma executes within 1 second on a computer with the Intel Xeon 5160, 3GHz processor. ■

7.3. Parameterization of center-unstable and center-stable manifolds at c_0 and c_9, respectively.

Lemma 7.4. *The following statements hold true:*

- *The center-stable manifold of PT at c_9 can be parameterized as a vertical disk in N_9 satisfying the cone conditions with respect to the quadratic form Q_9.*
- *The center-unstable manifold of PT at c_0 can be parameterized as a vertical disk in N_0 satisfying the cone conditions with respect to the quadratic form Q_0.*

The computer assisted proof of the above lemma is essentially the same as the proof of Lemmas 6.8 and 6.9 for the Hénon map. Therefore, we skip the details. The C++ program which verifies the assertion executes within 11 seconds on a computer with the Intel Xeon

5160, 3GHz processor. The most time-consuming part is the verification of the existence of covering relations for the projected sets in three-dimensional space.

We used the Taylor method of the order 20 and a variable time step when checking the covering relations and when integrating second order variational equations.

Proof of Theorem 7.1. We conclude the proof as in the Hénon map example. ∎

8. Implementation notes. In order to compute bounds for the Hénon map and the Poincaré map T_β and their derivatives we used the interval arithmetic [13], automatic differentiation [9], and the C^r-Lohner algorithm [21] developed at the Jagiellonian University by the CAPD group [8]. The C++ source files of the program with instructions on how it should be compiled and run are available online [19].

The program has been tested under several Linux distributions, including 32 and 64 bit architectures and the gcc compiler versions 4.1.2, 4.2.1, and 4.3.2 on the Intel Pentium IV, Intel Core 2 Duo, Intel Xeon, and the AMD Quad Core processors.

Appendix A. Proof of Remark 3.3.

In the proof we will produce on the plane (μ, x_1) the coordinate change of the form $(\mu, x_1) \mapsto (\nu(\mu), t(\mu, x_1))$. It is obvious that such a coordinate change preserves the form of the curve $s_\mu(x_1) = (x_1, 0)$.

The proof consists of several lemmas.

Lemma A.1. *The same assumptions as in Remark* 3.3 *hold. Assume that g is of class $\mathcal{C}^k$, with $k \geq 3$. Then there exists a local coordinate change $(\mu, x_1) \mapsto (\mu, t(\mu, x_1))$ of class $\mathcal{C}^k$, such that $t(\mu_0, 0) = 0$ and in the new coordinates g satisfies the following conditions for μ in some neighborhood of μ_0:*

$$g(\mu_0, 0) = 0, \quad \frac{\partial g}{\partial x_1}(\mu, 0) = 0,$$
$$\frac{\partial g}{\partial \mu}(\mu, 0) \neq 0, \quad \frac{\partial^2 g}{\partial x_1^2}(\mu, 0) \neq 0.$$

Proof. Observe that, since $\frac{\partial^2 g}{\partial^2 x_1}(\mu_0, 0) \neq 0$, from the implicit function theorem it follows that there exists a local function $\mu \mapsto x_1(\mu)$ of class $\mathcal{C}^{k-1}$, such that

$$\frac{\partial g}{\partial x_1}(\mu, x_1(\mu)) = 0, \quad x_1(\mu_0) = 0.$$

It is easy to see that if we set

$$t(\mu, x_1) = x_1 - x_1(\mu),$$

then our assertion is satisfied. ∎

Lemma A.2. *Assume that $f : \mathbb{R}^2 \to \mathbb{R}$ is a $\mathcal{C}^k$-function with $k > 2$, such that*

$$\frac{\partial f}{\partial x}(\mu, 0) = 0 \quad \forall \mu.$$

Then there exist functions $h : \mathbb{R}^2 \to \mathbb{R}$ of class $\mathcal{C}^{k-2}$ and $r : \mathbb{R} \to \mathbb{R}$, $r \in \mathcal{C}^k$, such that

$$f(\mu, x) = x^2 h(\mu, x) + r(\mu),$$

where $h(\mu,0) = 2\frac{\partial^2 f}{\partial x^2}(\mu,0)$ *and* $r(\mu) = f(\mu,0)$.

Proof. For any $\mathcal{C}^1$-function $w:\mathbb{R}\to\mathbb{R}$ it holds that

$$w(x) = w(0) + \int_0^1 w'(tx)dt\cdot x.$$

For fixed μ we apply the above formula to $w(x) = \frac{\partial f}{\partial x}(\mu,x)$ and then again to $w(x) = f(\mu,x)$ and we obtain

$$f(\mu,x) = f(\mu,0) + x^2\int_0^1\int_0^1 s\frac{\partial^2 f}{\partial x^2}(\mu,stx)dtds. \qquad \blacksquare$$

From the two above lemmas it follows that we can assume that our function $g(\mu,x_1)$ satisfies the following conditions:

$$g(\mu,x_1) = x_1^2 h(\mu,x_1) + r(\mu),$$
$$h(\mu_0,0)\neq 0, \quad r'(\mu_0)\neq 0.$$

Observe that since $r'\neq 0$ in the neighborhood of μ_0, we can use locally $r(\mu)$ instead of μ as the parameter. After this observation we can assume now that our function $g(\mu,x_1)$ satisfies the following conditions (now $\mu_0 = 0$):

$$g(\mu,x_1) = x_1^2 h(\mu,x_1) + \mu, \quad h(0,0)\neq 0. \tag{A.1}$$

To finish the proof we need the following lemma.

Lemma A.3. *Assume that g satisfies* (A.1). *Then there exists a local coordinate change in the neighborhood of* $(0,0)$ *of the form*

$$(\mu,x_1)\to(\mu,t = x_1(1+w(\mu,x_1))), \qquad w(0,0) = 0,$$

such that in these new coordinates we have

$$g(\mu,t) = at^2 + \mu, \tag{A.2}$$

where $a = h(0,0)$.

Proof. We have

$$h(\mu,x_1) = ax_1^2 + x_1^2 f(\mu,x_1), \qquad f(\mu,x_1) = O(|(\mu,x_1)|).$$

To obtain (A.2) w needs to satisfy the equation

$$ax_1^2 + x_1^2 f(\mu,x_1) + \mu = a(x_1(1+w(\mu,x_1)))^2 + \mu,$$

which is equivalent to the following condition:

$$f(\mu,x_1) = 2aw(\mu,x_1) + aw(\mu,x_1)^2. \tag{A.3}$$

We obtain the solution to (A.3) by application of the implicit function theorem to the following equation:

$$F(\mu,x_1,w) = f(\mu,x_1) - 2aw - aw^2 = 0.$$

Indeed we have $F(0,0,0) = 0$ and $\frac{\partial F}{\partial w}(0,0,0) = -2a\neq 0$. $\blacksquare$

REFERENCES

[1] Z. Arai, *Tangencies and the Conley index*, Ergodic Theory Dynam. Systems, 22 (2002), pp. 973–999.

[2] Z. Arai and K. Mischaikow, *Rigorous computations of homoclinic tangencies*, SIAM J. Appl. Dyn. Syst., 5 (2006), pp. 280–292.

[3] B. Bánhelyi, T. Csendes, B. Garay, and L. Hatvani, *A computer-assisted proof of Σ_3-chaos in the forced damped pendulum equation*, SIAM J. Appl. Dyn. Syst., 7 (2008), pp. 843–867.

[4] *CHOMP—Computational Homology Project*, http://chomp.rutgers.edu.

[5] M. Dellnitz and O. Junge, *GAIO*, http://math-www.uni-paderborn.de/∼agdellnitz/gaio.

[6] J.E. Fornaess and E.A. Gavosto, *Existence of generic homoclinic tangencies for Hénon mappings*, J. Geom. Anal., 2 (1992), pp. 429–444.

[7] J.E. Fornaess and E.A. Gavosto, *Tangencies for real and complex Hénon maps: An analytic method*, Experiment. Math., 8 (1999), pp. 253–260.

[8] Z. Galias, T. Kapela, M. Mrozek, P. Pilarczyk, D. Wilczak, P. Zgliczyński, and M. Zelawski, *CAPD—Computer Assisted Proofs in Dynamics, a Package for Rigorous Numerics*, http://capd.ii.uj.edu.pl.

[9] A. Griewank, *Evaluating Derivatives: Principles and Techniques of Algorithmic Differentiation*, Frontiers in Applied Mathematics 19, SIAM, Philadelphia, 2000.

[10] J. Guckenheimer and P. Holmes, *Nonlinear Oscillations, Dynamical Systems and Bifurcations of Vector Fields*, Appl. Math. Sci. 43, Springer-Verlag, New York, 1983.

[11] M. Hénon, *A two-dimensional mapping with a strange attractor*, Comm. Math. Phys., 50 (1976), pp. 69–77.

[12] H. Kokubu, D. Wilczak, and P. Zgliczyński, *Rigorous verification of cocoon bifurcations in the Michelson system*, Nonlinearity, 20 (2007), pp. 2147–2174.

[13] R.E. Moore, *Interval Analysis*, Prentice–Hall, Englewood Cliffs, NJ, 1966.

[14] J. Palis and F. Takens, *Hyperbolicity and Sensitive Chaotic Dynamics at Homoclinic Bifurcations*, Cambridge Studies in Advanced Mathematics 35, Cambridge University Press, Cambridge, UK, 1993.

[15] C. Robinson, *Bifurcation to infinitely many sinks*, Comm. Math. Phys., 90 (1983), pp. 433–459.

[16] J. Rohn, *Positive definiteness and stability of interval matrices*, SIAM J. Matrix Anal. Appl., 15 (1994), pp. 175–184.

[17] Q. Wang and L.-S. Young, *Strange attractors with one direction of instability*, Comm. Math. Phys., 218 (2001), pp. 1–97.

[18] Q. Wang and L.-S. Young, *Toward a theory of rank one attractors*, Ann. of Math. (2), 167 (2008), pp. 349–480.

[19] D. Wilczak, http://www.ii.uj.edu.pl/∼wilczak.

[20] D. Wilczak and P. Zgliczyński, *Topological method for symmetric periodic orbits for maps with a reversing symmetry*, Discrete Contin. Dyn. Syst., 17 (2007), pp. 629–652.

[21] D. Wilczak and P. Zgliczyński, *C^r-Lohner algorithm*, preprint.

[22] P. Zgliczyński, *Covering relations, cone conditions and the stable manifold theorem*, J. Differential Equations, 246 (2009), pp. 1774–1819.